Chemical shift optimized quantitative susceptibility mapping (csQSM)

Alexey V. Dimov[1,2], Tian Liu[3], Pascal Spincemaille[2], Jacob S. Ecanow[4,5], Huan Tan[6], Robert R. Edelman[4,7], and Yi Wang[1,2]

[1]Biomedical Engineering, Cornell University, Ithaca, NY, United States, [2]Radiology, Weill Cornell Medical College, New York, NY, United States, [3]MedImageMetric LLC, New York, NY, United States, [4]Radiology, NorthShore University HealthSystem, Chicago, IL, United States, [5]Radiology, University of Chicago Pritzker School of Medicine, Chicago, IL, United States, [6]Surgery (Neurosurgery), University of Chicago, Chicago, IL, United States, [7]Radiology, Northwestern University Feinberg School of Medicine, Chicago, IL, United States

TARGET AUDIENCE: Researchers interested in quantitative susceptibility mapping (QSM), water/fat separation and breast imaging.

PURPOSE: The goal of this study is to develop quantitative susceptibility mapping (QSM) for tissues with significant fat content. Although the total susceptibility field f_s in the presence of chemical shift can be estimated with various algorithms such as IDEAL[1], these nonlinear algorithms typically require 1) a good initialization for proper convergence and 2) a known chemical shift *a priori*. The chemical shift value f_1 varies among subjects and within organs of the same subject[2-4], causing errors in the subsequent determination of susceptibility. Additionally, a strong field inhomogeneity can make proper initialization challenging. Here we propose chemical shift QSM (csQSM) to address these two issues. The algorithm uses i) the fact that the chemical shift is the major cause for the field difference between neighboring voxels that have a significant difference in fat content and ii) an adaptive update of the chemical shift peak to achieve optimal data fitting.

csQSM ALGORITHM: Using the fact that the chemical shift is the major cause of a field jump of f_1 between neighboring voxels with very different fat content, the effects of the chemical shift from MRI signal can in a first approximation be removed by unwrapping field jumps $n/\Delta TE + mf_1^0$, where $n/\Delta TE$ is the standard 2π wrap-around with n an integer and ΔTE the echo spacing in data acquisition, and mf_1^0 is the chemical shift jump with m=0 or 1. This unwrapping was performed with the magnitude-guided field unwrapping algorithm[5] and uses an intial guess of the fat chemical shift value $f_1^0 = -3.5ppm \cdot \gamma B_0$ Hz. To avoid noise and partial volume effects, f_s is initialized to the background field f_b^0 from this unwrapped field obtained using the projection onto dipole field (PDF)[6] method.

f_s is then refined to provide an optimal fit for the data by adjusting the chemical shift. MRI data is modeled as $s(TE_n) = e^{-i2\pi f_s TE_n}(\rho_0 + \rho_1 e^{-i2\pi f_1 TE_n})$, where f_s (the total susceptibility field), ρ_0 and ρ_1 (water and fat contributions to the complex signal of a voxel at TE =0) are estimated by the IDEAL algorithm: $\rho_0^k, \rho_1^k, f_s^k = IDEAL[f_b^{k-1}, f_1^{k-1}], f_b^k = PDF[f_s^k], f_1^k = f_1^{k-1} + PCQSM[f_s^k - f_b^k]$, with k the iteration number. Here $PCQSM$ is the piece-wise constant QSM that allows estimation of relative chemical shift[7], which enables an efficient search path towards a minimal residue (Fig.1). Finally, this iteration is stopped when the f_1 update falls below a preset threshold of 1 Hz. The field f_s^k is then used to map susceptibility using MEDIN[5].

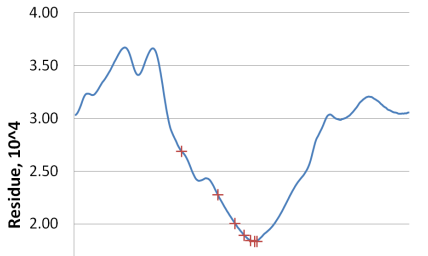

Fig.1 Dependence of model residue on the value of chemical shift; "+" indicate convergence path of the proposed algorithm

METHODS: csQSM was performed in phantoms and on in vivo data. Two types of phantoms were created: one of gelatin with embedded lard and another of excised bovine tissue containing intramuscular fat. Phantoms were imaged on a 3T MRI (GE Healthcare) system using an 8-channel head coil and a multi-echo 3D SPGR sequence (TE1 = 2.5ms, ΔTE= 2.25ms, 5 echoes, 3 acquisitions with TE1 incremented by 0.75ms, TR=34ms, FA=20°, BW=±62.50 kHz, scan time ~9 minutes).

With IRB approval and informed consent, two female volunteers with known calcifications were scanned on a 3T MRI system (Siemens AG Medical Solutions, Erlangen, Germany) using a 16 channel-coil (8 channels per breast) and a multi-echo 3D SPGR sequence (TE= 3.3ms, ΔTE=3.3ms, #TE=6, TR=35ms, FA=20°, BW=±62.50 kHz, and voxel size = 1.25×1.25×1mm^3).

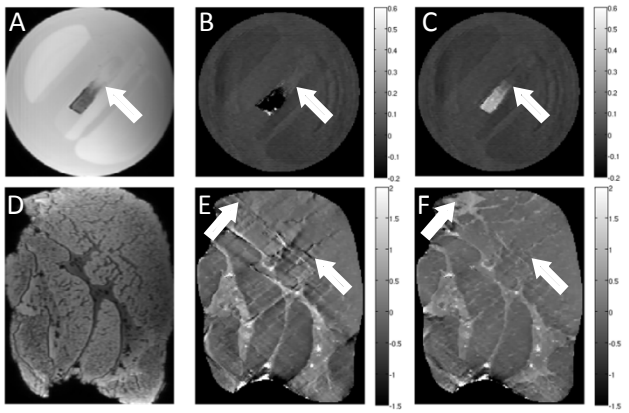

Fig.2 Magnitude images (A, D) and QSM maps of phantoms reconstructed without (B, E) and with (C, F) proposed algorithm

RESULTS: The phantom results are shown in Fig.2: the default chemical shift value ($f_1^0 = -3.5ppm$) failed to reconstruct QSM for the lard (Fig.2b, wrong susceptibility value $-0.6ppm$ relative to water) and bovine tissue (Fig.2e, streaking artifacts and wrong values); optimized chemical shift accurately reconstructed QSM (Fig.2c, lard susceptibility value $0.35ppm$ with $f_1 = -3.78ppm$; Fig.2f, no streaking with $f_1 = -3.64ppm$). csQSM was successfully performed on breast MRI: the optimized chemical shift ($f_1 = -3.9ppm$ in Fig.3b) overcame the artifacts in Fig.3a (default $f_1 = -3.5ppm$) and revealed calcifications, validated by the corresponding mammogram in the same patient (Fig.3c).

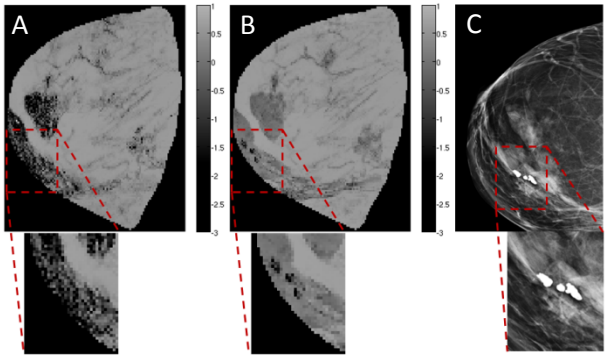

Fig.3 Minimal intensity projections of breast QSMs reconstructed without (A) and with (B) proposed algorithm compared with mammogram (C)

DISCUSSION AND CONCLUSIONS: Our preliminary data demonstrated that QSM can be obtained in tissues with significant fat content using a chemical shift optimized method (csQSM). This algorithm optimizes the chemical shift value by penalizing the discrepancy between data measured and data predicted from estimates of chemical shift fields and water and fat maps. Phantom validation and in vivo results suggest that the proposed chemical shift optimization significantly reduces streaking artifacts and provides improved susceptibility maps, enabling QSM applications beyond neuroimaging.

REFERENCES: 1. Reeder, S.B., et al. Magnet Reson Med 51, 35-45 (2004). **2.** Barany, M., et al. Magnet Reson Med 10, 210-226 (1989). **3.** Schick, F., et al. Magnet Reson Med 29, 158-167 (1993). **4.** Hernando, D., et al. Magnet Reson Med (2013). **5.** Liu, T., et al. Magnet Reson Med 69, 467-476 (2013). **6.** Liu, T., et al. NMR in biomedicine 24, 1129-1136 (2011). **7.** de Rochefort, et al. Magnet Reson Med 60, 1003-1009 (2008).